Clays and Clay Minerals, Vol. 60, No. 1, 63–75, 2012.

MINERAL COMPOSITIONAL TRENDS AND THEIR CORRELATIONS WITH PETROPHYSICAL AND WELL-LOGGING PARAMETERS REVEALED BY *QUANTA* + *BESTMIN* ANALYSIS: MIOCENE OF THE CARPATHIAN FOREDEEP, POLAND

JAN ŚRODOŃ AND TADEUSZ KAWIAK

Institute of Geological Sciences PAN, Senacka 1, 31002 Krakow, Poland

Abstract—This study uses the data from Miocene rocks of the Carpathian Foredeep to test the performance of the computer programs *QUANTA* and *BESTMIN* in aiding the interpretation of geophysical log data. These programs were designed to help trace trends in the mineral composition of rocks, the chemical composition of minerals, and the effects of these data on petrophysical and geophysical logging parameters. Chemical and X-ray diffraction data for 65 samples of shales, sandstones, and carbonates taken from cored wells in the molasse basin of the Carpathian Foredeep were processed. Compositional differences were detected between rocks sourced from the platform and rocks sourced from the Carpathians. Quartz, K-feldspar, and zircon were more abundant in the coarse-grained rocks (sandstones), while calcite, ankerite, siderite, pyrite, barite, halite, celestite, apatite, anatase, chlorite, 2:1 minerals, and organic matter were more abundant in the fine-grained rocks (shales). Plagioclase reached its maximum in coarse shales. Ankerite, chlorite, and dioctahedral 2:1 minerals had more Fe in the coarse-grained rocks. The dioctahedral 2:1 minerals in fine-grained rocks had a greater concentration of smectitic layers. This information permitted the precise calculation of grain density, porosity, adsorbed water, and some geophysical logging parameters. It also permitted the calibration of well-log response, in particular, the macroscopic neutron absorption cross-section (Σ_a) combined with the photoelectric absorption factor (P_e) or with P_e + Ca (calcium content, measurable in wells by spectroscopic techniques) with porosity and cation exchange capacity (CEC). The NaCl concentration in the pore waters was found to range from the values typical for seawater in shales to the freshwater level in clean sandstones.

Key Words—*BESTMIN*, Borehole Geophysics, CEC, Geochemical Logging, Grain Density, Illite-smectite, Log Calibration, *QUANTA*, Quantitative XRD, Porosity, Pore-water Chemistry.

INTRODUCTION

Characterization of petroleum reservoirs using well logs is commonly focused on the determination of porosity and water saturation. For clay-rich rocks (‘shaley sands’ and shales), the procedures are complicated by variations in the clay mineral chemistry, grain density, and cation exchange capacity (CEC) and associated electrical conductivity (Ellis and Singer, 2007).

A general strategy for conducting petrophysical analyses of shale lithologies has been presented elsewhere (Zorski *et al.*, 2011). No universal solution to this problem exists because correlations between the log data and rock parameters are affected by the mineral composition of the rock, which can be different in different basins. For each sedimentary basin, appropriate calibration must be performed, based on precise and detailed mineralogical, geochemical, and geophysical data acquired from core samples. The mineralogical and geochemical data acquired for the bulk-rock samples must be processed to assign the chemical components to particular minerals. Different approaches have been described and various mathematical procedures have been used to integrate the different types of data collected (*e.g.* Herron and Herron, 1997, 1998; Harvey *et al.*, 1998 and literature cited therein; Zorski *et al.* 2011). Fang *et al.* (1996) were the first to use genetic algorithms to calculate mineral composition of rocks from chemical data.

In the authors’ experience, the success of such calibration, *i.e.* the quality of the correlations produced, has depended heavily on the quality of mineralogical data, which are often less accurate and less precise than the chemical data and the geophysical measurements performed on the core samples. In particular, the quantification of clay minerals has proven difficult, as shown by the results of international contests (*e.g.* the ‘Reynolds Cup’ of The Clay Minerals Society, http://www.clays.org/SOCIETY%20AWARDS/RCintro.html), in which competitors analyze and report on the composition of aliquots of artificial rocks of known composition (*e.g.* Omotoso *et al.*, 2006). Another challenge is variable chemical composition of some mineral components, especially clays and carbonates, which may affect significantly the measured geophysical and petrophysical parameters. The present contribution tests tools (the *QUANTA* and *BESTMIN* programs) designed specifically to address both problems and is a

* E-mail address of corresponding author:
ndsrodon@cyf-kr.edu.pl
DOI: 10.1346/CCMN.2012.0600106

complementary study to those of Środoń (2009) and Zorski *et al*. (2011), which utilized some of the same *QUANTA* and *BESTMIN* data used here.

GEOLOGY AND MINERALOGY – BACKGROUND

The present study is based on 65 samples of clastic rocks from the Miocene marine molasse basin, termed the Carpathian Foredeep, developed between an orogenic belt (the Carpathians) and a platform (the East European Craton) (Figure 1). The samples represent the entire compositional range known for these rocks, from clean quartz sandstones to claystones and carbonates, and were taken from depths of 220–1040 m in three boreholes in the Dzików gas field (Table 1). The geology of the area and the relevant published mineralogical studies were described in an earlier paper (Środoń, 2009), which used the same sample set. The 2009 paper focused on quantifying the illite and smectite components of the rocks, mostly from CEC and EGME (ethylene glycol monoethyl ether) sorption measurements.

Sedimentological studies (S. Porębski, pers. comm., 2011) indicated that most of the section was sourced from the uplifting flysch Carpathians to the south, while the thick-bedded quartz arenites that occur at depths of ~900–1200 m were sourced from intrabasinal fault-bounded highs or from the cratonal (northern) margin of the molasse basin. A recent study of sandstone composition from the area (Kuberska *et al*., 2008) reported quartz, including rare authigenic overgrowths, calcite, ankerite, feldspars, phosphates, micas, illite, illite-smectite, chlorite, and kaolinite. Quartz, K-feldspar, plagioclase, anatase, calcite, dolomite/ankerite, siderite, pyrite, dioctahedral 2:1 minerals, chlorite, kaolinite, and corundum were detected (Środoń, 2009) (the corundum was contamination from the grinding rollers in a sandstone sample).

METHODS

The rocks were crushed in a hand mortar to pass a 0.4 mm sieve, and then divided with a hand splitter into portions for X-ray diffraction (XRD) and chemical analysis. Quantitative mineral compositions were obtained for all samples using the XRD patterns of ZnO-spiked random preparations (THERMO X'Tra

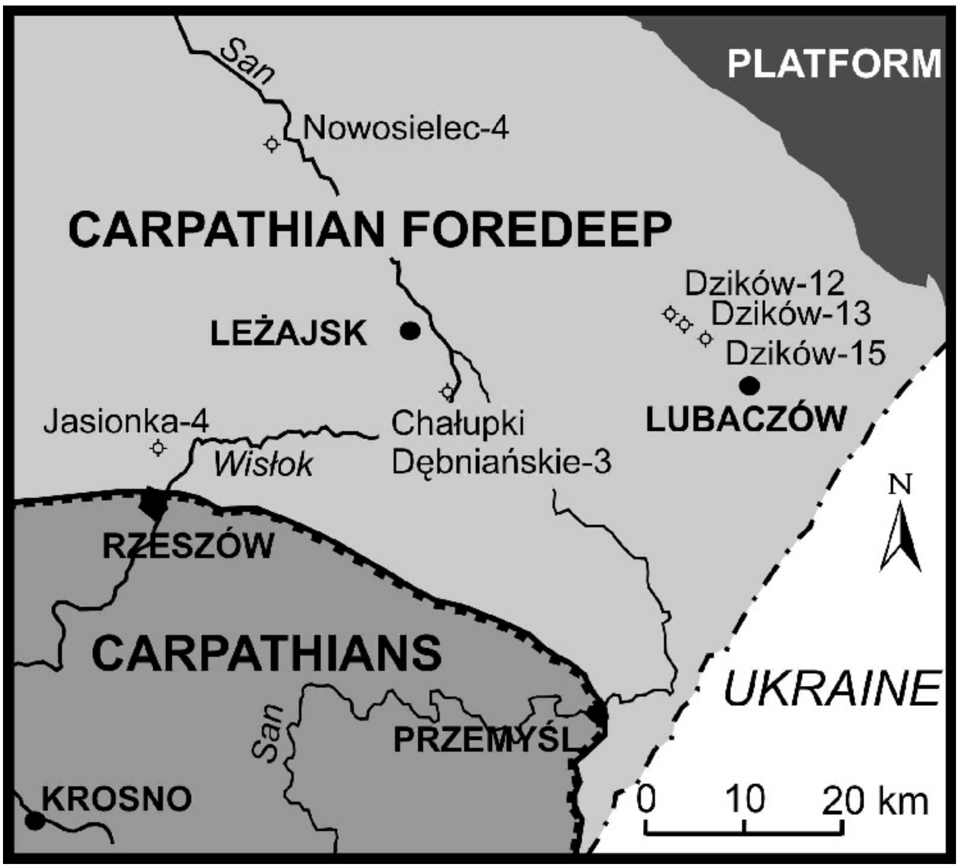

Figure 1. Study area showing the location of the Dzików gas field (reproduced from Figure 9 of Środoń (2009) with the kind permission of the Mineralogical Society of Great Britain & Ireland).

https://doi.org/10.1346/CCMN.2012.0600106 Published online by Cambridge University Press

Table 1. *BESTMIN* evaluation of the mineral composition of the rocks studied (wt.% relative to air-dried rock), presented as mean values of seven groups. The samples were assigned to groups based on their 2:1 mineral and calcite contents. The 2:1 minerals include all dioctahedral 2:1 minerals (illite, glauconite, muscovite, and illite-smectite), Org stands for organic matter content, and H_2O is the molecular water present in the rock in the air-dried state.

Group	Quartz	K-feld-spar	Plagio-clase	Zircon	Pyrite	Barite	Halite	Celes-tite	Apatite	Ana-tase	Calcite	Fe-Do-lomite	Side-rite	Kaoli-nite	Chlor-ite	2:1 mineral	Org	H_2O	SUM
Carpathians-sourced																			
Shale 1	27.6	1.9	5.0	0.029	0.54	0.06	0.26	0.04	0.29	0.64	7.8	3.6	1.2	1.1	6.0	35.0	1.07	3.52	95.59
Shale 2	41.7	2.0	6.5	0.035	0.32	0.05	0.28	0.04	0.26	0.56	6.7	3.8	0.9	1.4	4.1	24.5	0.81	2.30	96.43
Shale 3	53.1	2.9	7.9	0.038	0.28	0.05	0.23	0.03	0.24	0.46	6.2	3.4	0.5	1.0	2.6	16.0	0.42	1.41	97.01
Carbonate 1	53.2	3.0	6.5	0.035	0.11	0.04	0.12	0.03	0.16	0.32	15.1	4.8	0.4	0.9	1.1	10.0	0.13	0.74	96.96
Sandstone 1	68.1	4.0	7.0	0.043	0.10	0.04	0.11	0.02	0.16	0.33	4.3	1.9	0.3	1.0	0.7	8.3	0.13	0.69	97.37
Platform-sourced																			
Carbonate 2	28.1	0.3	0.0	0.05	1.38	0.01	0.37	0.10	0.11	0.17	58.6	0.2	0.1	1.2	0.0	5.7	0.18	0.47	98.98
Sandstone 2	86.7	1.0	0.3	0.05	0.22	0.01	0.21	0.02	0.08	0.18	5.0	0.1	0.1	0.4	0.1	4.9	0.10	0.48	99.85

diffractometer, 45 kV, 40 mA, 2–65°2θ, 2 s counting/0.02°2θ step, 0.9/1.6/1.6/0.3 mm + 2 Soller slit system) and the *QUANTA* computer program (Mystkowski *et al.*, 2002; Omotoso *et al.*, 2006), based on the method of Środoń *et al.* (2001).

QUANTA is a hybrid of the single-peak and the whole-pattern fitting approaches to quantitative XRD analysis. It fits the whole pattern of a sample with the experimental patterns of pure standards using genetic algorithms.

Different weights can be assigned to selected angular ranges during the fitting procedure. This unique feature of the *QUANTA* program allows the user to take advantage of the variable sensitivity of different XRD reflections to the chemical and structural variability of a given mineral (Środoń *et al.*, 2001). The accuracy of *QUANTA* analyses has been tested in round-robin competitions (*e.g.* Omotoso *et al.*, 2006).

Major-element analysis was performed by SGS Minerals, Canada, who used the X-ray fluorescence (XRF) technique on glass discs obtained by fusion of lithium tetraborate-lithium metaborate. NIST 70a (potassium feldspar) and 76a (burnt refractory) standards were used to check the accuracy of these analyses.

Trace elements were analyzed by inductively coupled plasma mass spectrometry of solutions of fused samples at Actlabs, Canada. Additional determinations by different techniques for this study were of B, S, F, and N (Actlabs); Cl, organic C, and H_2O^+ (SGS Minerals); H_2O^-, CEC_{rock}, and total specific surface area ($TSSA_{\mathrm{rock}}$) (Krakow laboratory of the ING PAN, Poland). Details of the techniques were given by Środoń (2009). Summaries of the *QUANTA* results and chemical analyses were given by Zorski *et al.* (2011).

The mineral data from *QUANTA* and the chemical data were analyzed jointly using *BESTMIN*, a program written in Java by Krzysztof Mystkowski, which determines the elemental compositions of common sedimentary rock minerals that are characterized by isomorphic substitutions (clays and micas, feldspars, carbonates, and zeolites), and uses the results to calculate accurately the grain density, the TSSA, and several other petrophysical and geophysical rock parameters (Środoń *et al.*, 2006). See Figure 2 for the general scheme of *BESTMIN* refinement. The chemical and the XRD data were first put on a common basis (air-dried state) by correcting the chemical data for water lost during drying at 100°C before chemical analysis (H_2O^-). Chemical data, as available, were then used to calculate minor contents of certain compositionally invariant minerals if they were undetected by XRD, or to correct concentrations of minerals that were detected by XRD. For instance, BaO is assigned to barite, SrO to celestite, TiO_2 to anatase, Zr to zircon, P_2O_5 to apatite, S to pyrite and sulfates, and Cl to halite. The compositions of compositionally invariant minerals were subtracted from the totals. A genetic algorithm was then used to evaluate

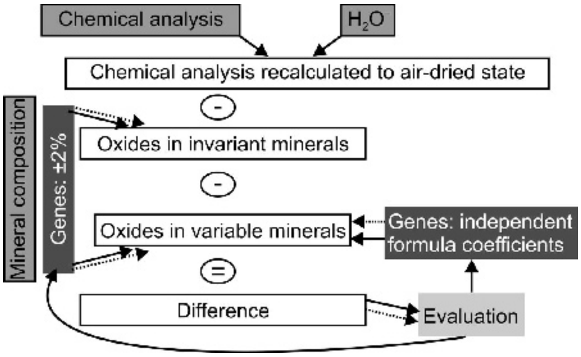

Figure 2. General scheme of *BESTMIN* operation.

the structural formulae of variable minerals. The values undergoing optimization (genes) are independent coefficients of structural formulae of the variable minerals and the mineral percentages from *QUANTA*. All genes were varied within pre-selected ranges, representing either the variability of a given value known from natural environments or an arbitrary error range in the case of *QUANTA* values (typically ±2% absolute).

BESTMIN uses certain simplifications. For example, it assumes only the most feasible and volumetrically important isomorphic substitutions: Sr is assigned to aragonite but not to calcite, Mg to siderite but not to other carbonates, *etc*. The dioctahedral 2:1 mineral fraction of the rock (muscovite + illite + glauconite + illite-smectite + smectite) is considered as a single 'mineral,' consistent with *QUANTA*, which also quantifies these minerals as a group, and the CEC_{rock} measurement is applied to aid refinement of the 2:1 mineral composition using the approach based on Środoń *et al*. (1992):

$$\frac{2EXCH}{MW} = \frac{CEC_{2:1}}{100000} \tag{1}$$

Assuming that all of the CEC of the rock comes from its 2:1 mineral we can write:

$$CEC \times \%2{:}1 = CEC \times (100 - \mathrm{H_2O}) \tag{2}$$

thus:

$$EXCH = \frac{CEC_{\mathrm{rock}} \times MW \times (100 - H_2O^-)}{\%2:1 \times 200000} \tag{3}$$

and

$$FIX = Q_{\mathrm{i}} \times \left(1 - \frac{EXCH}{Q_{\mathrm{s}}}\right) \tag{4}$$

where: *EXCH* and *FIX* are the exchangeable and fixed cation contents (in moles of charge per half unit cell) of the molecular water-free dioctahedral 2:1 minerals in the rock, respectively; Q_s and Q_i are the corresponding layer charges; *MW* is the molecular weight; $CEC_{2:1}$ and CEC_{rock} are the cation exchange capacities (meq/100 g) of the molecular water-free 2:1 minerals in the rock and of the whole water-free rock, respectively; %2:1 is the weight percent of the molecular water-free 2:1 minerals in the air-dried rock; and H_2O^- is the amount of water released (wt.%) from the sample between room temperature and 110ºC, which corrects for the fact that CEC values are measured at 110ºC and %2:1 in air-dried conditions.

MW, Q_i, and Q_s are considered as genes in *BESTMIN*. As for all other genes, their values can also be fixed if their values are known from independent sources. Reducing the number of variable genes improves the reliability of the *BESTMIN* solutions.

The sum of the absolute values of differences between the measured and calculated oxide mass fractions is used as a criterion for the goodness of fit. Once the optimization is finished, the gene values are used in the calculation of refined *MW* and refined volume of the unit cell needed for the grain-density calculation. The unit-cell parameters, sensitive to chemical composition, are refined by means of experimental regressions. For carbonates, *a* and *c* parameters are calculated by the regressions of Chang *et al*. (1998), McCarty *et al*. (2006), and the authors of the program (siderite):

$$a = 0.4641 - 0.006 \times \mathrm{Mg} + 0.0077 \times \mathrm{Mn}$$
$$c = 1.5379 - 0.036 \times \mathrm{Mg} + 0.0255 \times \mathrm{Mn}$$

For feldspars, mean values of orthoclase/microcline and albite/anorthite (Deer *et al.*, 1997) were used. The albite/anorthite ratio was established from refined chemistry and the orthoclase/microcline ratio was set as 1 if specific data were not available. For chlorites, a simplified version of the Wiewióra and Wilamowski (1996) regression for the *b* parameter was applied, and for dioctahedral 2:1 minerals the regression for *b*, established by the authors of the program (Środoń et al, 2006), was used:

$$b = 6 \times (0.0131 \times \mathrm{Fe} + 1.4971)$$

Grain densities resulting from these refinements allowed recalculation of mass fractions into volume fractions. The calculations of various petrophysical and geophysical parameters followed, based on generally available formulae (*e.g.* Ellis and Singer, 2007). The macroscopic neutron absorption cross-sections (Σ_a, given in capture units, cu) were calculated from the microscopic cross-sections of nuclei provided by Drozdowicz and Krynicka (1995). The photoelectric absorption factor (P_e) was calculated for each mineral from its elemental composition. This was done using an MS-*Excel*® spreadsheet provided by T. Zorski (pers. comm., based on Bertozzi *et al*., 1981). Grain density was also used for calculating bulk-rock porosity *via* a standard equation from the experimentally measured bulk density (data from Woźnicka, 2007)).

The parameters characterizing the dioctahedral 2:1 mineral fraction of the rock were calculated following Środoń *et al*. (1992 – equations 5 and 6; and 2000 – equation 7) and Środoń and McCarty (2008 – equations 8 and 9):

$$N = \frac{1}{\left(1 - \frac{FIX}{Q_i}\right)} \tag{5}$$

$$\%S_{2:1} = \frac{100}{N} \tag{6}$$

$$r = \left(\frac{7728 - (18368 \times Nt) + (10988 \times (Nt)^2)}{\pi}\right)^{0.5} \tag{7}$$

$$TSSA_{2:1} = \frac{2000}{\rho_{2:1}} \times \left(\frac{1}{Nt} + \frac{1}{r}\right) \tag{8}$$

$$H_2O_{2:1} = \frac{100}{1 + \frac{\rho_{2:1}}{2t_w\rho_w \times \left(\frac{1}{Nt}+\frac{1}{r}\right)}} \tag{9}$$

where: N is the area-weighted mean number of 2:1 layers in fundamental particles, $\%S_{2:1}$ is the percentage of smectitic interlayers in the 2:1 mineral (including crystal basal surfaces regarded as smectitic: see Środoń *et al*., 1992), r is the mean radius of the fundamental particles (in nm), t is the mean thickness of a layer in the fundamental particle (in nm, close to 1), $TSSA_{2:1}$ is the total specific surface area of the 2:1 fraction (m^2/g), $\rho_{2:1}$ is the density of the 2:1 fraction (g/cm^3), ρ_w is the density of water (g/cm^3, close to 1), t_w is the mean thickness of a monolayer of water on the surfaces of 2:1 minerals (close to 0.25 nm), and $H_2O_{2:1}$ is the wt.% of water present on the surfaces of the 2:1 mineral fraction as a monomolecular layer (approximately the water content of the air-dried clay; Środoń and McCarty, 2008).

The dioctahedral 2:1 mineral fraction content (Table 1) and its characteristics obtained *via* equations 6, 8, and 9 (Table 2) were used in *BESTMIN* to calculate the corresponding parameters of the bulk rock (Table 3), under the assumption that essentially all of the surface area of the rock came from the dioctahedral 2:1 fraction. This assumption restricts the use of *BESTMIN* to rocks which are free of significant amounts of other components with large TSSA values, *e.g.* kerogen, zeolites, opal, or amorphous phosphates. Only trioctahedral smectite can be refined separately and its effect on the bulk-rock parameters $TSSA_{rock}$, $\%S_{rock}$, and H_2O_{rock} can be accounted for. The calculation is approximate only, ignoring the differences in densities between illite, smectite, and the remaining part of the rock, but it does provide useful characteristics of the bulk rock.

BESTMIN can perform its calculations on the inputs from a single sample or from a set of samples (under the

Table 2. *BESTMIN* evaluation of the chemical composition of minerals with variable composition, presented as mean coefficients of the structural formulae for seven groups of rocks. The additional values listed for the 2:1 mineral are: N – the mean number of layers in fundamental particles, $\%S$ – the smectite layer content, and *TSSA* – the total specific surface area (m^2/g).

Group	Fe-dolomite	Siderite				K feldspar	Plagioclase	Chlorite						2:1 minerals										
	Fe^{2+}	Fe^{2+}	Mg	Mn	Ca	K	Na	Si	^{IV}Al	^{VI}Al	Fe^{3+}	Fe^{2+}	Mg	Si	^{IV}Al	^{VI}Al	Fe^{3+}	Mg	K	Na	Ca	N	$\%S_{2:1}$	$TSSA_{2:1}$ (m^2/g)
Carpathians-sourced																								
Shale 1	0.25	0.63	0.12	0.19	0.06	0.92	0.77	2.78	1.22	0.77	0.45	1.78	3.00	3.45	0.55	1.59	0.27	0.15	0.48	0.20	0.01	1.94	52	380
Shale 2	0.24	0.63	0.10	0.22	0.05	0.90	0.74	2.77	1.23	0.79	0.44	2.08	2.69	3.42	0.58	1.57	0.29	0.13	0.51	0.19	0.00	2.12	49	355
Shale 3	0.26	0.63	0.10	0.22	0.05	0.93	0.74	2.77	1.23	0.79	0.44	2.38	2.39	3.41	0.59	1.54	0.32	0.14	0.53	0.18	0.01	2.29	47	338
Carbonate 1	0.37	0.58	0.02	0.38	0.02	0.92	0.77	2.89	1.11	0.76	0.35	3.22	1.66	3.40	0.60	1.33	0.49	0.18	0.63	0.14	0.01	2.85	37	263
Sandstone 1	0.27	0.64	0.07	0.27	0.03	0.92	0.73	2.87	1.13	0.79	0.34	2.94	1.93	3.36	0.64	1.39	0.47	0.14	0.63	0.14	0.01	2.82	37	260
Platform-sourced																								
Carbonate 2	0.20	0.97	0.00	0.03	0.00	0.85	n.a	n.a	n.a	n.a	n.a	n.a.	n.a.	3.68	0.32	0.73	0.91	0.35	0.46	0.07	0.07	1.95	54	386
Sandstone 2	0.48	0.73	0.11	0.12	0.03	0.79	0.77	2.70	1.30	0.77	0.53	3.82	0.88	3.64	0.36	0.64	0.92	0.45	0.67	0.07	0.03	3.24	33	227

https://doi.org/10.1346/CCMN.2012.0600106 Published online by Cambridge University Press

Table 3. *BESTMIN* evaluation of petrophysical and logging parameters of the studied rocks, presented as mean values of seven rock groups. $TSSA_{\mathrm{rock}}$ – the total specific surface area, $\%S_{\mathrm{rock}}$ – the smectite content, Q_v – the conductivity term of the Waxman-Smits equation, P_e – the photoelectric absorption factor, GR_{API} – the gamma ray response of the rock, V_{sh} – the volume fraction of all hydrogen-bearing minerals calculated on a water-free basis, Σ_a – the macroscopic neutron absorption cross-section of the dry rock matrix.

Group	$TSSA_{\mathrm{rock}}$ (m^2/g)	$\%S_{\mathrm{rock}}$	Grain density, dry (g/cm^3)	Grain density, 110ºC (g/cm^3)	Grain density, air-dry (g/cm^3)	Porosity, dry (%)	Porosity, 110ºC (API) (%)	Porosity, air-dry (%)	Q_v	P_e	GR_{API}	V_{sh}	$\Sigma_{a,}$ dry (cu)	Rock SiO_2/oxygen ratio	NaCl in pore water (ppm)
Carpathians-sourced															
Shale 1	140	19	2.74	2.70	2.58	18.27	17.03	13.00	1.39	3.66	97.47	0.44	28.86	0.94	24273
Shale 2	90	12	2.72	2.69	2.61	22.54	21.74	19.33	0.68	3.29	80.75	0.31	23.07	0.95	16354
Shale 3	53	7	2.70	2.69	2.64	26.59	26.08	24.75	0.30	2.96	65.03	0.20	18.39	0.96	9628
Carbonate 1	26	4	2.71	2.69	2.67	14.75	14.38	13.62	0.43	3.11	47.56	0.12	14.21	0.96	13377
Sandstone 1	23	3	2.68	2.67	2.65	28.43	28.11	27.57	0.11	2.54	49.83	0.10	13.06	0.97	3974
Platform-sourced															
Carbonate 2	17	2	2.71	2.71	2.69	15.96	15.75	15.28	0.23	4.35	28.86	0.09	12.96	0.93	28785
Sandstone 2	13	2	2.67	2.66	2.65	29.42	29.13	28.84	0.05	2.29	19.14	0.05	10.45	0.99	6442

assumption that they contain minerals with the same chemical composition across the set). *BESTMIN* performance has been tested on artificial rock samples and found to be satisfactory (Środoń *et al.*, 2006). In particular, *BESTMIN* improved XRD quantitative estimates. A measured CEC_{rock} value is essential for evaluating the 2:1 component properly. The accuracy of solutions is improved if some variables are evaluated independently and fixed during execution of the program. A rigorous error analysis has not been implemented at this stage of the program development.

RESULTS

Modeling details

All samples were modeled in *BESTMIN* individually and also as sets that have similar mineral composition (Table 1). Samples sourced from the Carpathians were arbitrarily split into three 'shale' sets and a 'sandstone' set, based on quartz content, used in this case as a proxy for grain size, and a 'carbonate' set, based on elevated calcite content. Samples sourced from the platform were split into 'sandstone' and 'carbonate' sets, based on quartz and calcite contents.

BESTMIN modeling was performed using the *QUANTA* mineral contents both raw and normalized to 100%. In accordance with the findings of Środoń *et al.* (2009) and Środoń (2009), Q_i was fixed at $1.00/O_{10}(OH)_2$, and Q_s was treated as variable or fixed at 0.4. Measured CEC_{rock} values were also used as input data. All these approaches (individual *vs*. set modeling, raw *vs*. normalized *QUANTA* data, variable *vs*. fixed Q_s) produced very similar trends. In particular, set analyses and averaging the relevant individual analyses produced very similar results. The paragraphs below describe results for the individual sample analyses performed for the normalized mineral contents and fixed Q_s.

Trends in the mineral composition of rocks

BESTMIN analysis quantified minor components that were undetected by XRD: zircon, barite, halite, celestite, apatite, anatase, and organic matter (Table 1). The mineral contents separated the studied sample set into two groups, corresponding to different provenance, indicated by sedimentological characteristics (Table 1). The samples from depths >900 m form the sandstone 2 and carbonate 2 sets and represent the rocks sourced from the craton. Their common characteristics are very low K-feldspar, plagioclase, chlorite, ankerite, and siderite contents. The major difference between the carbonate 2 and the sandstone 2 set was the quartz/calcite ratio and the pyrite content. No shale samples were sourced from the craton.

The samples from depths of <900 m represented the rocks were sourced from the Carpathian orogen. Very clear gradual compositional trends can be traced from the most fine-grained set, shale 1, to the coarsest set,

https://doi.org/10.1346/CCMN.2012.0600106 Published online by Cambridge University Press

sandstone 1 (the position of carbonate 1 among the Carpathian-sourced sample sets is based on its clay content: Table 1). Only the quartz, K-feldspar, and zircon contents increased systematically from shale 1 to sandstone 1. Plagioclase increased in shales, but reached its maximum content in the coarsest shale (shale 3), and was lower in the sandstone and the carbonate. The modeled contents of most of the other minerals (calcite, ankerite, siderite, pyrite, barite, halite, celestite, apatite, anatase, chlorite, and 2:1 mineral) and organic matter decreased. Exceptions to this rule were elevated calcite and ankerite contents in carbonate 1. Kaolinite varied little in abundance at a level close to the detection limit (1%).

All the detected mineralogical trends are controlled by the lithology. Dispersion of data presented in synthetic form in Table 1 is illustrated in Figure 3. The investigated set of samples was continuous with respect to the mineral composition, and % quartz and %2:1 minerals may serve as equivalent proxies for the grain size.

Vertical variation in the profiles was also investigated. The only clear correlation of the mineral content *vs*. depth detected was an elevated ankerite content in shales from the 600–750 m depth interval.

Trends in the chemical composition of variable minerals

Clear trends in the chemical composition of ankerite, siderite, chlorite, and the 2:1 mineral group were observed with increasing grain size in the samples from depths of <900 m, while the compositions of K-feldspar and plagioclase were nearly constant (Table 2). The Fe content of 0.24–0.37 atoms per structural formula confirmed the XRD identification of ankerite. The Fe content increased slightly, but carbonate 1 contained a clearly elevated value. Siderite was characterized by large Mn contents (0.16–0.38 per structural formula). The Mg and Ca contents decreased while Mn increased. Carbonate 1 contained the extreme values of all four of these elements. In chlorite, Fe increased while Mg decreased. The trend was very strong, leading from the Mg-dominated chlorite in shales 1 and 2 to Fe dominated in carbonate 1 and sandstone 1. As in the cases of ankerite and siderite, carbonate 1 contained the extreme values.

In 2:1 minerals, ^{IV}Al, Fe, and K increased, while ^{VI}Al and Na decreased. Mg stayed nearly constant, except for a slightly elevated value in carbonate 1. Ca was almost absent from the exchange positions of the 2:1 minerals. The ^{IV}Al and Fe contents were clearly larger and of Mg were smaller than typical for illite-smectite from bentonites (Środoń *et al*., 1986; 2009). The increase in K (fixed cations) corresponded to thicker fundamental particles (bigger *N*), less expandability (smaller %*S*), and smaller *TSSA* values of the 2:1 fraction of coarser rocks (Table 2; see equations 5, 6, 8).

BESTMIN estimates of the compositions of most minerals from >900 m samples must be regarded with caution because of the very small abundances of these minerals. Only the data for the relatively abundant 2:1 mineral can be considered as reliable. They indicate a composition quite different from the <900 m samples: much smaller ^{IV}Al and ^{VI}Al contents, much larger Fe and Mg, and smaller Na contents, and much more Ca.

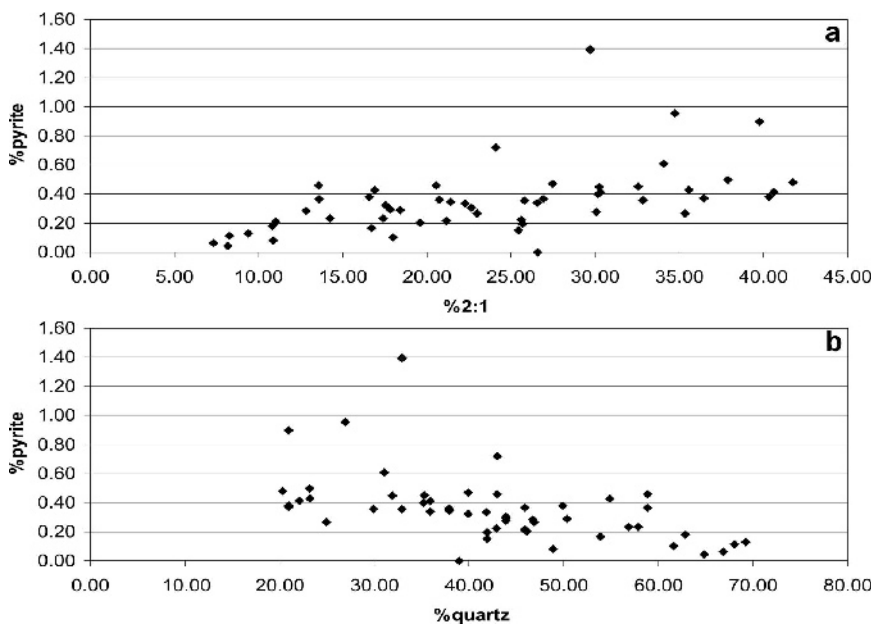

Figure 3. Example of mineral trends controlled by lithology: the pyrite content in individual samples plotted *vs*. (a) the 2:1 minerals content and (b) the quartz content.

https://doi.org/10.1346/CCMN.2012.0600106 Published online by Cambridge University Press

The 2:1 minerals from the carbonate differed from the sandstone clay in its much larger smectite content.

All the compositional features detected using the group analysis (Table 2) could also be demonstrated by plotting the *BESTMIN* chemical data obtained for individual samples *vs*. %2:1 mineral, which is a good indicator of the grain size of the rocks studied. Typical correlations are presented in Figure 4. The most apparent compositional differences visible for small %2:1 values correspond to the sandstone 2 and carbonate 2 sets.

Effect of mineral trends on petrophysical and geophysical rock parameters

The most important parameters calculated by *BESTMIN* for the seven selected rock groups (Table 3) revealed that the first two, surface area of the rock and smectite content of the rock, are interrelated and dependent on both the content (%2:1) and the characteristics (%$S_{2:1}$) of the 2:1 mineral fraction, which both increase in fine-grained rocks (Tables 1 and 2). As a result, the surface area of the rock and the smectite content of the rock decrease with increasing grain size much faster than do the corresponding characteristics of the 2:1 fraction.

Grain densities are calculated in three versions: (1) no water on clay surfaces (dry); (2) water remaining on clay surfaces at 110ºC (based on the data of Środoń and McCarty, 2008), and counted as part of the rock skeleton and not part of the pore space (110ºC); and (3) with monomolecular water layer on clay surfaces (based on equation 9) and counted as part of the skeleton (air-dried). Porosities calculated from such grain densities correspond to (1) total dry porosity; (2) porosity measured in standard laboratory conditions; and (3) total porosity corrected for the monomolecular water layer on clay surfaces. Dry grain densities decrease and porosities increase with decreasing clay content, with the exception of the carbonate samples, which do not obey this rule because the grain density of carbonates is significantly greater than that of quartz. Air-dried densities increase with decreasing clay content, which has a profound effect on the calculation of porosities of fine-grained rocks (5% difference for Shale 1 listed in Table 3). The geophysical parameters include: the conductivity term of the Waxman-Smith equation (Q_v), the photoelectric absorption factor (P_e), the gamma ray response of the rock (GR_{API}), the macroscopic neutron absorption cross-section of the rock matrix (Σ_a, given in capture units, cu), and the volume fraction of all hydrogen-bearing minerals calculated on a water-free basis (V_{sh}). *BESTMIN* also calculates some geochemical parameters such as SiO_2/oxygen ratio or NaCl concentration in pore water. All these parameters evolve gradually with increasing grain size of the rock. Some of the results listed in Table 3 will be considered in more detail below.

Density and porosity. *BESTMIN* calculates grain density from the mineral composition data, and then uses these values to calculate porosity if the bulk density data have been introduced. In the present study, bulk-density data obtained by direct mass and volume measurement (Woźnicka, 2007: GeoPyc 1360 instrument, measured

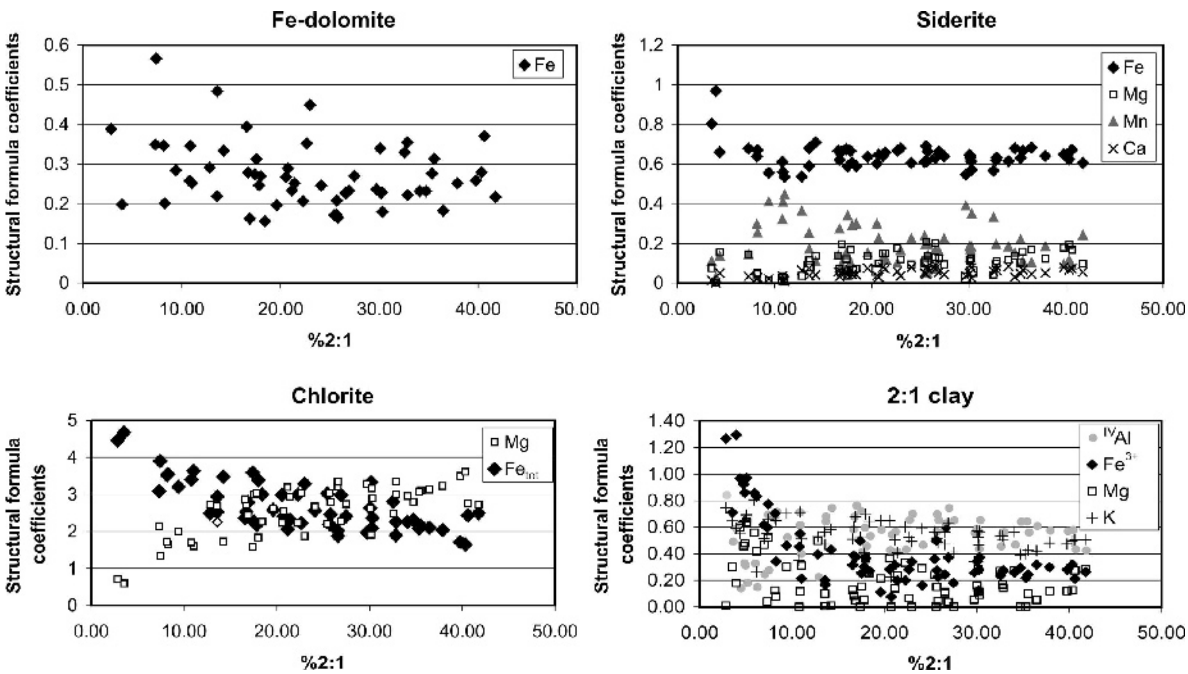

Figure 4. Trends in chemical composition of selected minerals (coefficients of structural formulae per half unit cell), established by *BESTMIN* analyses of individual samples.

https://doi.org/10.1346/CCMN.2012.0600106 Published online by Cambridge University Press

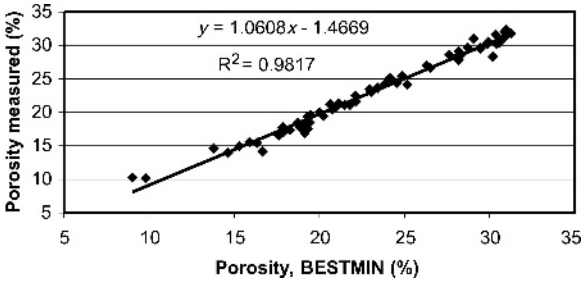

Figure 5. Correlation of porosity calculated from laboratory measurements of bulk density plus grain density and porosity calculated by *BESTMIN* using measured bulk density values.

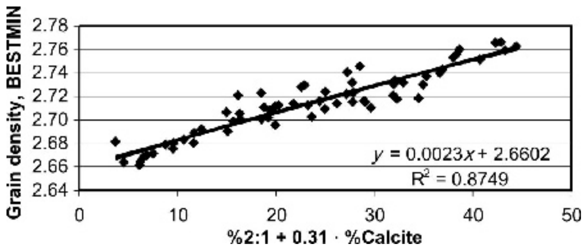

Figure 7. The best experimental correlation of practical use between grain density calculated by *BESTMIN* and the sample mineral composition.

at the Oil and Gas Institute, Kraków) were introduced into *BESTMIN*. Direct measurements of the grain density by helium pycnometry (AccuPyc 1330, measured in the Oil and Gas Institute, Kraków) and the resulting porosity data were used as a reference, in order to evaluate *BESTMIN* performance.

Porosities (Φ) calculated by *BESTMIN* from its own calculated grain density and calculated for comparison from the measured grain density data are very close but not identical (Figure 5). The differences are small and can be mostly attributed to the grain-density data (Figure 6). *BESTMIN* values reveal clear correlation with the rock-mineral composition as expected, while the measured values are not correlated, which can be traced to a relatively large error associated with this measurement (±0.03 g/cm^3 declared by the laboratory). For this reason, *BESTMIN* porosity calculations are considered to be more accurate, and are used below. Part of the problem with the measured values may result from the residual water present in the samples and resultant reduction of the measured grain density. *BESTMIN* handles this situation by calculating the grain density for samples dried at 110ºC, thus containing such residual water. If these data are used, the correlation with the measured values is improved further (compare the regression in Figure 5):

$$\Phi_{meas} = 1.024 * \Phi_{BESTMIN} + 0.1125 \qquad R^2 = 0.99$$

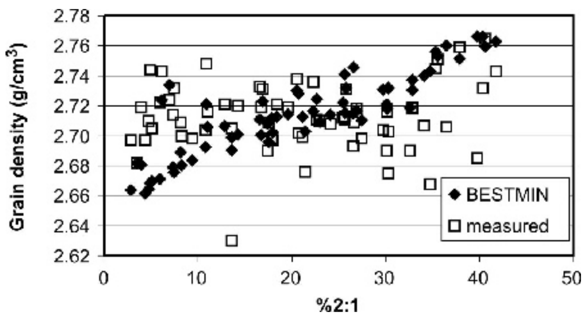

Figure 6. Grain density measured in the laboratory and calculated by *BESTMIN*, plotted *vs.* the mass fraction of 2:1 minerals.

The correlation of the *BESTMIN* grain density and %2:1 mineral in Figure 6 is disturbed by the effect of variable amounts of calcite, which has significantly greater grain density than quartz. If this factor is taken into account, the correlation can be improved significantly (Figure 7). The latter correlation may be useful for calculating porosity from the grain density obtained directly from the geophysical log data (neutron and neutron-gamma tools), as %2:1 can be evaluated quite accurately from the neutron absorption cross section, Σ_a, (Figure 8) and % calcite from %CaO (Figure 9). The results of calculating porosity *via* the standard porosity equation using the grain density obtained from these experimental regressions (Figures 7–9) are compared in Figure 10 to the direct *BESTMIN* calculation.

Portions of total pore space are occupied by different types of water. *BESTMIN* data (total specific surface area and grain density) permit calculation of the amount of water forming a monomolecular layer on the $TSSA_{rock}$. The relationship between total porosity and the part of that porosity that is surface water (Figure 11a) revealed that rocks with high porosities (sandstones) have a smaller amount of surface water (both absolute and relative) than rocks with low porosities (shales). The samples with anomalously low water porosity/total porosity ratios are carbonates. In the most clay-rich rocks, up to 40% of total porosity is occupied by the surface water (Figure 11b). The relationship in Figure 11b is not linear but concave because in the clay-rich rocks 2:1 minerals are more smectitic (Table 2).

Total specific surface area. *BESTMIN* calculates $TSSA_{rock}$ from the clay mineral contents and *TSSA* of

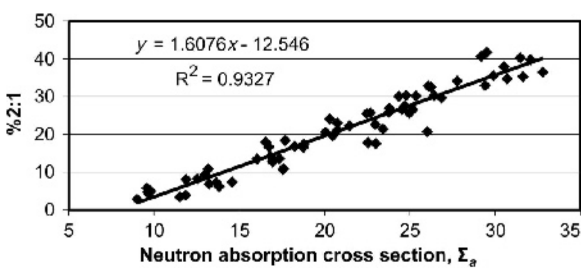

Figure 8. Correlation of the neutron absorption cross section, Σ_a, calculated by *BESTMIN* and the 2:1 minerals content.

https://doi.org/10.1346/CCMN.2012.0600106 Published online by Cambridge University Press

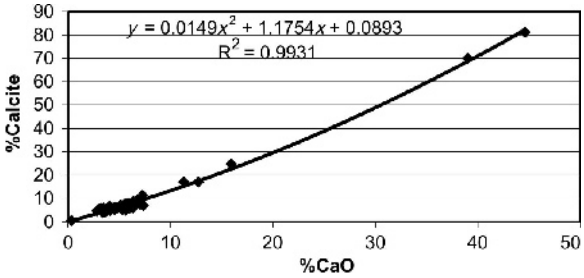

Figure 9. Correlation of the measured %CaO and the calcite content.

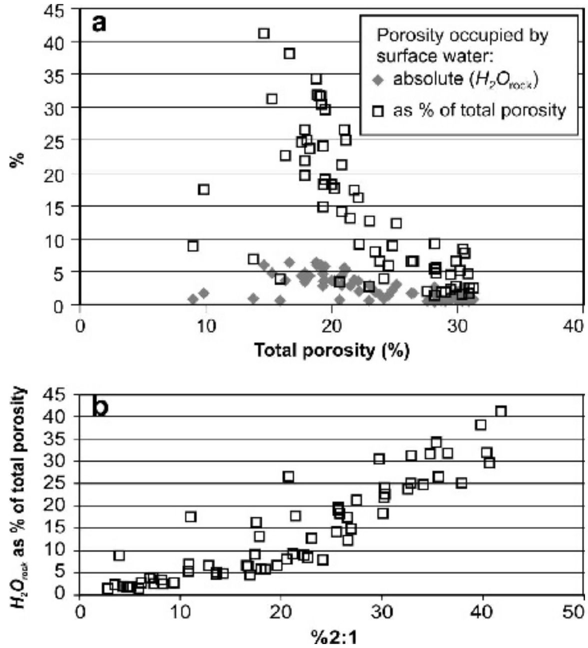

Figure 11. Volume fractions (%) of water bound as monomolecular film on mineral surfaces (H_2O_{rock}), plotted (a) *vs.* total porosity as absolute values and as a percentage of total porosity; (b) *vs.* %2:1 minerals as a percentage of the total porosity.

these clays. For kaolinite and chlorite, fixed values of 25 m^2/g are assumed (average based on literature data) and for the 2:1 mineral the value calculated by *BESTMIN via* equation 8 is used. The accuracy of *BESTMIN* calculations can be checked by comparing the $TSSA_{\mathrm{rock}}$ value calculated with that measured by the EGME sorption technique (Figure 12).

CEC. Evaluation of CEC_{rock} from the geophysical log data is an important step in interpretation of the data, as knowledge of CEC_{rock} is essential for evaluation of effective porosity (Ellis and Singer, 2007; Zorski *et al.*, 2011). *BESTMIN* modeling demonstrates strong correlations of CEC_{rock} with Σ_a and GR_{API} (Figure 13a,b), which can be used for evaluating CEC_{rock} from the logging data. Both correlations are non-linear. In the case of Σ_a the curvature reflects the fact that $CEC_{2:1}$ increases in fine-grained rocks (more smectitic composition: *cf*. Table 2), as Σ_a reveals a linear correlation with the %2:1 minerals (Figure 8), which is explained by the linear correlation of %2:1 minerals and the boron content (Figure 14), and the fact that the Σ_a of boron is ~3300–50,000 times greater than the Σ_a of major elements (Si, Al, K ...) in sedimentary rocks. The %2:1 minerals-boron content correlation has been documented by analogous methods in the Carboniferous shales of Donbas (Środoń and Paszkowski, 2011).

In the case of the correlation of CEC_{rock} with GR_{API} (Figure 13b), the curvature is stronger, which reflects a non-linear relationship of GR_{API} and %2:1 fraction (Figure 15a). In the sample set studied, GR_{API} is closely proportional to $\%K_2O$, except for four samples representing one bed sourced from the craton (Figure 15b). Thus, the non-linearity shown in Figure 13b reflects the combination of two effects of varying layer composition of the 2:1 fraction (Table 2), which affects the two parameters in opposite senses (more smectitic clay means greater $CEC_{2:1}$ but less K_2O and thus lower GR_{API}). An additional minor effect results from the elevated K-feldspar content in coarser rocks (Table 1).

The relationship of P_e and CEC_{rock} is more complex (Figure 16a). The general trend reflects systematically changing chemical composition from sandstones (low

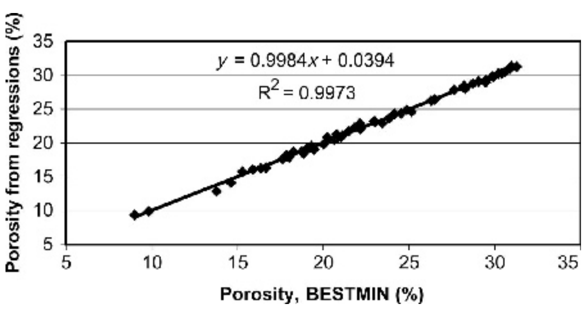

Figure 10. Comparison of the porosity calculated from Σ_a and %CaO, using the regressions from Figures 6–8, with the porosity calculated by *BESTMIN*.

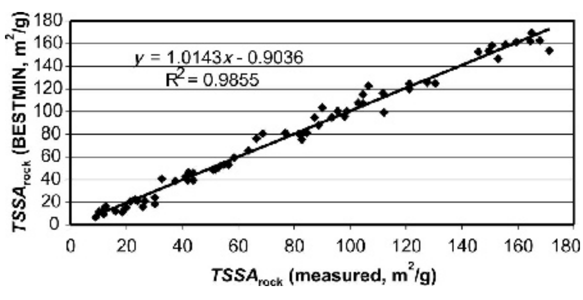

Figure 12. Verification of *BESTMIN* calculations: total specific surface area (TSSA) calculated by *BESTMIN vs.* values measured by the EGME technique (data from Środoń, 2009).

https://doi.org/10.1346/CCMN.2012.0600106 Published online by Cambridge University Press

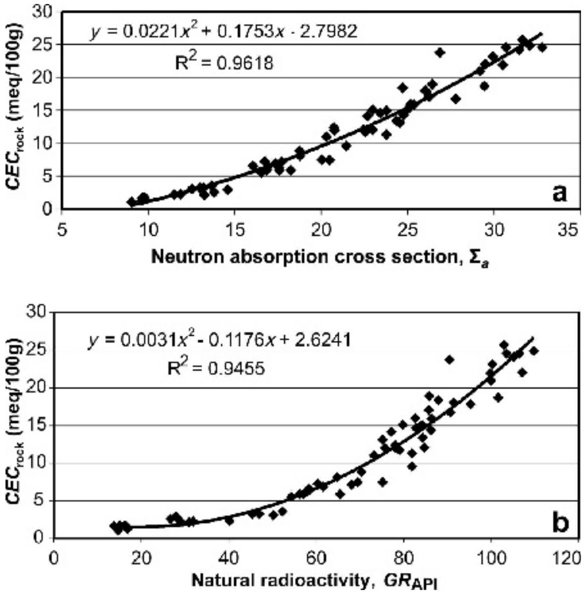

Figure 13. Correlations of measured (Środoń, 2009) cation exchange capacity of the rock, CEC_{rock}, with (a) the neutron absorption cross section, Σ_a, and (b) the natural radioactivity as GR_{API} (both calculated by *BESTMIN*).

P_{e}) to shale 1 (high P_{e}), and the positive anomalies from this trend can be traced to the elevated calcite or calcite + ankerite content in carbonates (Tables 1, 3). The quality of the correlation, which is comparable to GR_{API} *vs*. CEC_{rock}, can be obtained if %CaO is introduced as a second variable aside from P_{e} (Figure 16b). The single point outside the trend represents a sample with anomalously high siderite content. Figure 16b offers an opportunity to evaluate grain density (Figure 7) without the neutron-gamma measurement of %CaO, as its value can be obtained from Σ_a and P_{e} by combining the experimental regressions from Figures 13a and 16b.

Pore-water composition

BESTMIN assigns all measured Cl to NaCl and uses porosity to calculate NaCl concentration in pore water, under the assumption that all pore spaces were filled with water and that the monolayer of water on the

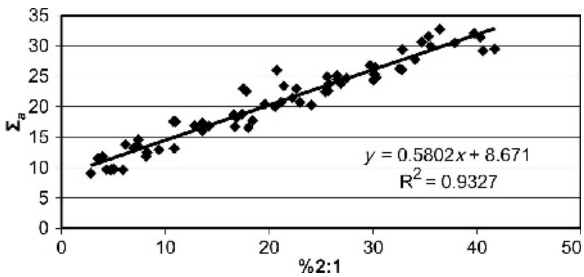

Figure 14. Correlation of the mass fraction of 2:1 minerals with (a) the neutron absorption cross section, Σ_a, and (b) the boron content.

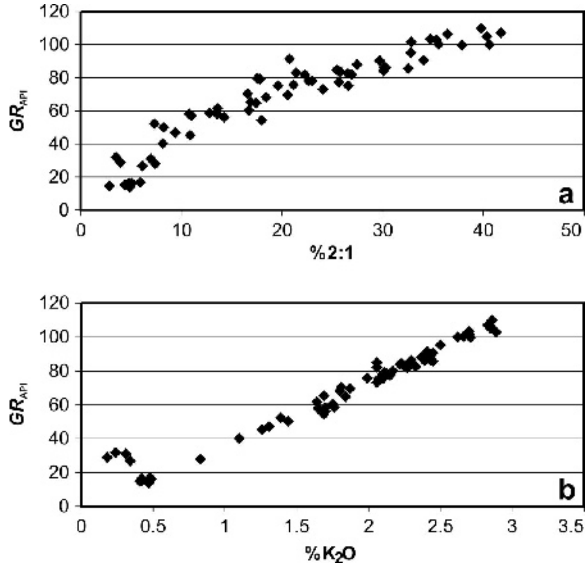

Figure 15. Correlations of the natural radioactivity as GR_{API} with (a) the mass fraction of 2:1 minerals and (b) $\%K_2O$.

$TSSA_{\mathrm{rock}}$ does not contain Cl. If these data are plotted against %2:1 minerals (Figure 17), a clear pattern appears: NaCl concentration increases from a few thousand ppm, *i.e.* the level characteristic of fresh waters, in sandstones, to ~24,000 ppm, typical of marine water in shales. This evolution is paralleled by the modeled composition of the exchange cations in smectitic interlayers: from Na in shales to significant amounts of Ca in the cleanest sandstones (Table 2). The carbonates are exceptional, having elevated NaCl concentrations, comparable to fine shales, despite the small clay content.

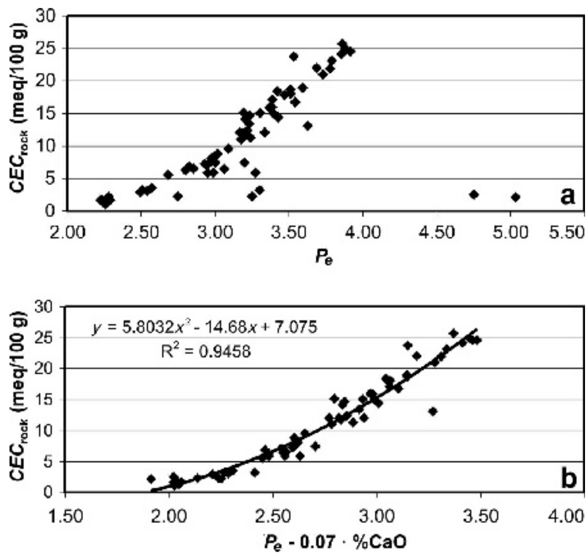

Figure 16. Correlations of measured (Środoń, 2009) CEC_{rock} with (a) the photoelectric absorption factor, P_{e}, and (b) P_e – 0.07%CaO (to account for excess Ca in carbonate rocks).

https://doi.org/10.1346/CCMN.2012.0600106 Published online by Cambridge University Press

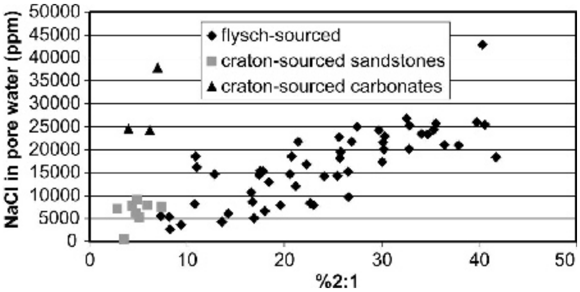

Figure 17. Correlation of the NaCl concentration in pore water calculated by *BESTMIN* with the mass fraction of 2:1 minerals.

Calculated NaCl concentration is inversely correlated with porosity (Table 3). Fine shales and carbonate 2 may well preserve the original marine pore water, while in the coarser rocks, which are more permeable, the pore water composition may have been affected by the movement of diagenetic pore fluids and has been affected by the drilling and core-cleaning procedures (S. Kowalska, pers. comm.). In any case, *BESTMIN* provides information about the pore-water composition in shales, useful for water-saturation calculations (Waxman-Smits formula: Zorski *et al*., 2011).

DISCUSSION AND CONCLUSIONS

The calculations performed by *BESTMIN* have been verified positively using two independently evaluated parameters: porosity (Figure 5) and TSSA (Figure 12). *QUANTA-BESTMIN* data, both mineral and chemical, confirmed different sources of sediments, indicated by the sedimentological studies.

Most of the trends detected in the mineral compositions of rocks can be assigned to sedimentary sorting or early diagenetic processes. Some, such as the decrease in plagioclase in sandstone 1 or the more Fe-rich composition of chlorite and ankerite in sandstone 1 and carbonate 1, will not be understood without a microscope study. Larger amounts of Fe in the 2:1 mineral probably reflect greater glauconite contents, as has been reported from these sandstones (Kuberska *et al*., 2008). Smaller %*S* values in the 2:1 mineral of sandstones determined by *BESTMIN* correspond to more illitic 2:1 mineral composition in sandstones, identified by XRD (Środoń, 2009), and agree with the estimates made by Środoń (2009) using different techniques. The presence of quite illite-rich illite-smectites, including the R1 variety, in the craton-sourced sandstones and carbonates (Środoń, 2009) is not surprising, given the level of diagenesis of the Mesozoic rocks forming the Miocene basin basement in the area (Kowalska, 2008).

The 2:1 mineral group is one of the most important components of clastic rocks, responsible for many of their properties. *BESTMIN* offers a unique technique for the chemical characterization of this component. Whether the characteristics detected are specific to the basin studied or are more widespread remains to be seen. This type of data has not been available so far.

Information on the composition of the exchange cations on smectitic surfaces (Table 2) and on the composition of pore water in contact with these surfaces (Figure 17) were obtained without any chemical extraction procedures, which may affect both values (*e.g.* Sayles and Mangelsdorf, 1977). Both values are interesting from the electric log-interpretation point of view (Waxman-Smits equation: Ellis and Singer, 2007).

The present study proves the utility of *BESTMIN* as an effective tool for calculating well-logging parameters and correlating them with various rock characteristics, which are to be measured by the logging techniques. Using this approach, laboratory measurements of petrophysical and logging parameters (grain density, Σ_a, P_e, GR_{API}, *etc*.), performed routinely for calibration purposes (see Zorski *et al*., 2011), can be avoided or at least kept to a minimum. In particular the grain density evaluation by *BESTMIN* is believed to be more accurate than the laboratory measurement. This study offers a strategy for calculating grain density from the logging data that is alternative to the traditional approach (evaluating sand, carbonate, and clay: see Zorski *et al*., 2011) and may find application in improving sonic velocity models. The *BESTMIN* approach to evaluating the pore-water salinity may find a potential use in reservoirs with variable resistivity. The detailed characteristics of the 2:1 mineral provided by *BESTMIN* allow evaluation of the fraction of pore space occupied by bound water.

ACKNOWLEDGMENTS

The present study was financed by the Polish Ministry of Science and Higher Education within the scientific network 'Nuclear methods for borehole geophysics.' JS thanks Dr Tomasz Zorski for his assistance with the P_e and Σ_a calculations during the development of the *BESTMIN* program, and Dr Leszek Chudzikiewicz for his help in editing figures. Permission from Chevron to use their proprietary *QUANTA* and *BESTMIN* programs is much appreciated. Meticulous comments by Eric Eslinger as the reviewer and J.M. Wampler as the associate editor helped considerably with the language and the clarity of presentation.

REFERENCES

Bertozzi, W., Ellis, D.V., and Wahl, J.S. (1981) The physical foundation of formation lithology logging with gamma-rays. *Geophysics*, **46**, 1439–1455.

Chang, L.L.Y., Howie, R.A., and Zussman, J. (1998) *Rock-Forming Minerals*, Vol. 5B. The Geological Society, London.

Deer, W.A., Howie, R.A., and Zussman, J. (1997) *Rock-Forming Minerals*, Vols 1–4. The Geological Society, London.

Drozdowicz, K. and Krynicka, E. (1995) Thermal neutron diffusion parameters in homogeneous mixtures. Report INP No.1694/PN, The H. Niewodniczański Institute of Nuclear Physics, Krakow, Poland.

Ellis, D.V. and Singer, J.M. (2007) *Well Logging for Earth Scientists*. Springer, Berlin, 692 pp.

Fang, J.H., Karr, C.L., and Stanley, D.A. (1996) Transformation of geochemical log data to mineralogy using genetic algorithms. *The Log Analyst*, **37**, 26–31.

Harvey, P.K., Brewer, T.S., Lovell, M.A., and Kerr, S.A. (1998) The estimation of modal mineralogy: a problem of accuracy in core-log calibration. Pp. 25–38 in: *Core-Log Integration* (P.K. Harvey and M.A. Lovell, editors). Special Publication **136**, Geological Society, London.

Herron, M.M. and Herron, S.L. (1997) Log interpretation parameters determined from chemistry, mineralogy and nuclear forward modeling. *Proceedings of International Symposium of the Society of Core Analysts*, Calgary, Alberta, 8–10 September 1997, pp. 1–12.

Herron, M.M. and Herron, S.L. (1998) Quantitative lithology: open and cased hole application derived from integrated core chemistry and mineralogy database. Pp. 81–95 in: *Core-Log Integration* (P.K. Harvey and M.A. Lovell, editors). Special Publication **136**, Geological Society, London.

Kowalska, S. (2008) Clay mineral evidence for the transition from diagenesis to anchimetamorphism in the Upper Proterozoic and Cambrian rocks of the Małopolska Massif. PhD thesis, Institute of Geological Sciences PAN, Kraków, Poland, 316 pp. (in Polish).

Kuberska, M., Kozłowska, A., and Maliszewska, A. (2008) Sandstone cements in the Polish and Ukrainian part of the Miocene Carpathian Foredeep. 1st Polish Geological Congress, Kraków, Poland, Abstracts, p. 61 (in Polish).

McCarty, D.K., Drits, V.A., and Sakharov, B. (2006) Relationship between composition and lattice parameters of some sedimentary dolomite varieties. *European Journal of Mineralogy*, **18**, 611–627.

Mystkowski, K., Środoń, J., and McCarty, D.K. (2002) Application of evolutionary programming to automatic XRD quantitative analysis of clay-bearing rocks. The Clay Minerals Society 39th Annual Meeting, Boulder, Colorado, USA, Abstracts.

Omotoso, O., McCarty, D.K., Hillier, S., and Kleeberg, R. (2006) Some successful approaches to quantitative mineral analysis as revealed by the 3rd Reynolds Cup contest. *Clays and Clay Minerals*, **54**, 748–760.

Sayles, F.L. and Mangelsdorf, P.C., Jr. (1977) The equilibration of clay minerals with seawater: exchange reactions. *Geochimica et Cosmochimica Acta*, **41**, 951–960.

Środoń, J. (2009) Quantification of illite and smectite and their layer charges in sandstones and shales from shallow burial depth. *Clay Minerals*, **44**, 421–434.

Środoń, J. and McCarty, D.K. (2008) Surface area and layer charge of smectite from CEC and EGME/H_2O retention measurements. *Clays and Clay Minerals*, **56**, 142–161.

Środoń, J. and Paszkowski, M. (2011) Role of clays in diagenetic history of nitrogen and boron in the Carboniferous of Donbas (Ukraine). *Clay Minerals*, **46** 561–582.

Środoń, J., Morgan, D.J., Eslinger, E.V., Eberl, D.D., and Karlinger, M.R. (1986) Chemistry of illite/smectite and end-member illite. *Clays and Clay Minerals*, **34**, 368–378.

Środoń, J., Elsass, F., McHardy, W.J., and Morgan, D.J. (1992) Chemistry of illite-smectite inferred from TEM measurements of fundamental particles. *Clay Minerals*, **27**, 137–158.

Środoń, J., Eberl, D.D., and Drits, V.A. (2000) Evolution of fundamental-particle size during illitization of smectite and implications for reaction mechanism. *Clays and Clay Minerals*, **48**, 446–458.

Środoń, J., Drits, V.A., McCarty, D.K., Hsieh, J.C.C., and Eberl, D.D. (2001) Quantitative XRD analysis of clay-rich rocks from random preparations. *Clays and Clay Minerals*, **49**, 514–528.

Środoń, J., Mystkowski, K., McCarty, D.K., and Drits, V.A. (2006) BESTMIN: a computer program for refining the quantities and the chemical composition of clays and other mineral components of fine-grained rocks. International Conference "Clays and Clay Minerals", Pushchino, Russia, Abstracts, p. 41.

Środoń, J., Zeelmaekers, E., and Derkowski, A. (2009) The charge of component layers of illite-smectite in bentonites and the nature of end-member illite. *Clays and Clay Minerals*, **57**, 649–671.

Wiewióra, A. and Wilamowski, A. (1996) The relationship between composition and *b* for chlorite. *Geologica Carpathica – Series Clays*, **5**, 79–87.

Woźnicka, U. (2007) Geochemical-mineralogical models constructed using data from advanced techniques of borehole geophysics. Part I. Report INP No.2008/AP, The H. Niewodniczański Institute of Nuclear Physics, Kraków, Poland (in Polish).

Zorski, T., Ossowski, A., Środoń, J., and Kawiak, T. (2011) Evaluation of mineral composition and petrophysical parameters by the integration of core analysis data and wireline well log data: the Carpathian Foredeep case study. *Clay Minerals*, **46**, 25–45.

(*Received 13 April 2011; revised 17 January 2012; Ms. 565; A.E. J.M. Wampler*)